

# A model of surface wind field in a tropical cyclone over Indian seas

B. K. BASU and S. K. GHOSH

Meteorological Office, New Delhi

(Received 6 February 1986)

**सार** — भारतीय समुद्रों पर उत्पन्न चक्रवात के अन्दर सतही दाब पार्श्विका के गणितीय स्वरूप को चार चक्रवातों के साथ तुलना करके निकाला गया है। इस दाब पार्श्विका को निवेश रूप में प्रयोग करके, चक्रवात क्षेत्र के अन्दर पवन के क्षैतिज वितरण को चार बलों अर्थात् दाब-प्रवणता, अभिकेन्द्री, घर्षण तथा कोरियोलिस बल की एक अर्ध-साम्यावस्था मानकर आंकित रूप में प्राप्त किया गया है। चक्रवात की गति के कारण, पवन क्षेत्र में समानता की भी जांच पड़ताल की गई है। अधिकतम वायु की त्रिज्या तथा तूफान के स्थानान्तरण जैसे निवेश प्राचलों को स्थिर मानकर, चक्रवातों के ऐसे 50 मामलों में अधिकतम हवा के मानों को परिकलित किया गया है, जिनके प्रेक्षितमान साहित्य में उपलब्ध हैं। परिकलित मॉडल तथा प्रेक्षित मानों के बीच मूल माध्य वग (आर. एम. एस.) त्रुटि 11 नॉट से कम पाई गई है।

यह आशा है कि यह मॉडल, चक्रवात के भीतर सतह-पवन क्षेत्र का अनुमान लगाने के लिये यथार्थ विधि प्रदान करेगा।

**ABSTRACT.** A mathematical form of the surface pressure profile within a cyclone forming over Indian seas is derived by comparison with observations of four cyclones. Using this pressure profile as input, the horizontal distribution of wind within a cyclone field is numerically obtained by assuming a quasi-equilibrium of four forces, viz., pressure-gradient, centrifugal, friction and coriolis forces. Asymmetry in the wind-field due to motion of the cyclone is also investigated. Keeping input parameters like radius of maximum wind and speed of translation of the storm fixed, values of maximum wind are computed for fifty cases of cyclones for which observed values are available in literature. The r.m.s. error between model computed and observed values is found to be less than 11 knots.

It is expected that the model will provide an objective method of estimating the surface wind field within a cyclone.

## 1. Introduction

Over Indian seas cyclonic storms occur almost every year. Such storms cause widespread devastation on land mainly due to the strong surface wind, heavy rain and storm surge associated with them. Over sea areas the strong surface wind and associated waves are the two most important factors influencing the weather routing of ships. In addition, the surface wind field inside a cyclone is an essential input for any storm surge model. Hence, for forecasting effects of cyclones both on land and sea it is important to know the distribution of surface wind inside the cyclone field.

Observations of surface wind within a cyclone field are few over Indian seas as ships avoid regions of disturbed weather and dropwindsonde observations are not available on routine basis due to lack of reconnaissance aircraft. As a result the detailed structure of wind field inside a cyclone over Indian seas is not known except for some basic facts like asymmetry of wind field with respect to the direction of motion, existence of a region of maximum wind & empirical relationship between maximum wind and pressure drop. In the present paper an attempt is made to deduce theoretically the structure of surface wind field inside cyclones from the basic principles of dynamics.

A parcel of air moving inside a stationary cyclone field will be subjected to four forces, namely, the pressure gradient force, the centrifugal force, the coriolis force and the friction force. In addition to these, another force arising due to the translation of the pressure field will have to be taken into account in the case of a moving cyclone. Out of these five forces the pressure gradient force is independent of wind speed; coriolis and storm motion forces depend linearly on the wind speed and centrifugal and friction forces vary as the square of the wind speed. In polar coordinates [Fig. 1(a)], tangential and normal components of the equation of motion can be written (Myers and Malkin 1961) as

$$\frac{dV}{dt} = \frac{1}{\rho} \frac{\partial p}{\partial r} \sin \beta + \frac{1}{\rho r} \frac{\partial p}{\partial \theta} \cos \beta - k_s V^2 \quad (1)$$

$$V \frac{d\beta}{dt} = \frac{1}{\rho} \frac{\partial p}{\partial r} \cos \beta - \frac{1}{\rho r} \frac{\partial p}{\partial \theta} \sin \beta$$

$$- fV - \frac{V^2}{r} \cos \beta + \frac{V V_{e1}}{r} \sin \theta - k_n V^2 \quad (2)$$

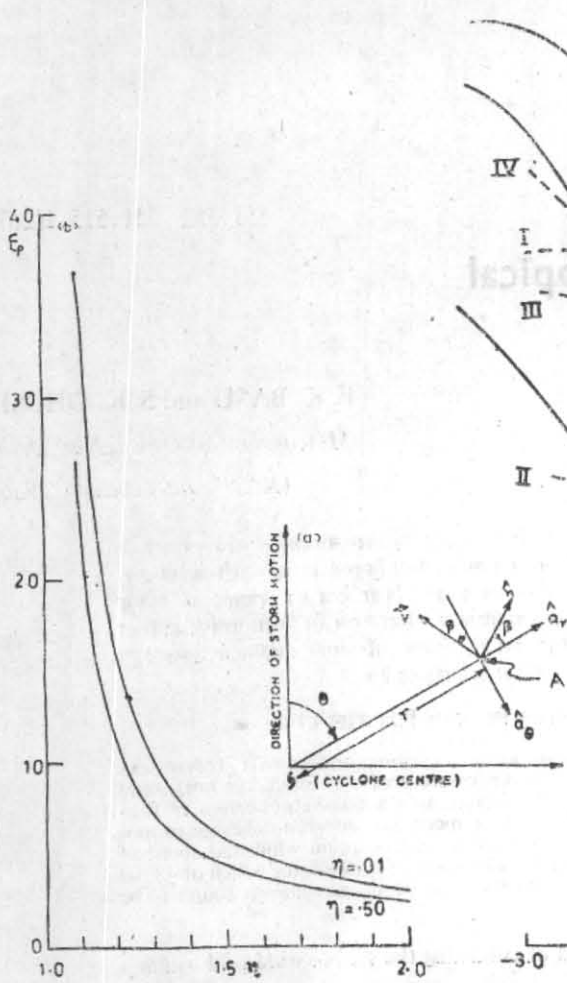


Fig. 1(a). Direction of vectors and angles used to describe the wind at point A within the cyclone field

Fig. 1(b). Variation of normalized distance  $\left(\xi = \frac{r}{a}\right)$  for different values of  $n$

where

- $r$  = radial distance from centre of the cyclone
- $\theta$  = azimuthal angle measured clockwise from direction of motion (taken as  $0^\circ$ )
- $V$  = wind speed at a location  $(r, \theta)$  w.r.t. centre
- $p$  = pressure at surface at location  $(r, \theta)$
- $\rho$  = air density near surface
- $\beta$  = cross-isobaric angle measured anticlockwise
- $f$  = Coriolis parameter
- $V_e$  = storm speed

$k_s, k_n$  = coefficients relating tangential and normal components of friction to square of wind speed.

In the case when speed and direction of movement of the storm are known the above equations relate instantaneous acceleration to the variation of pressure

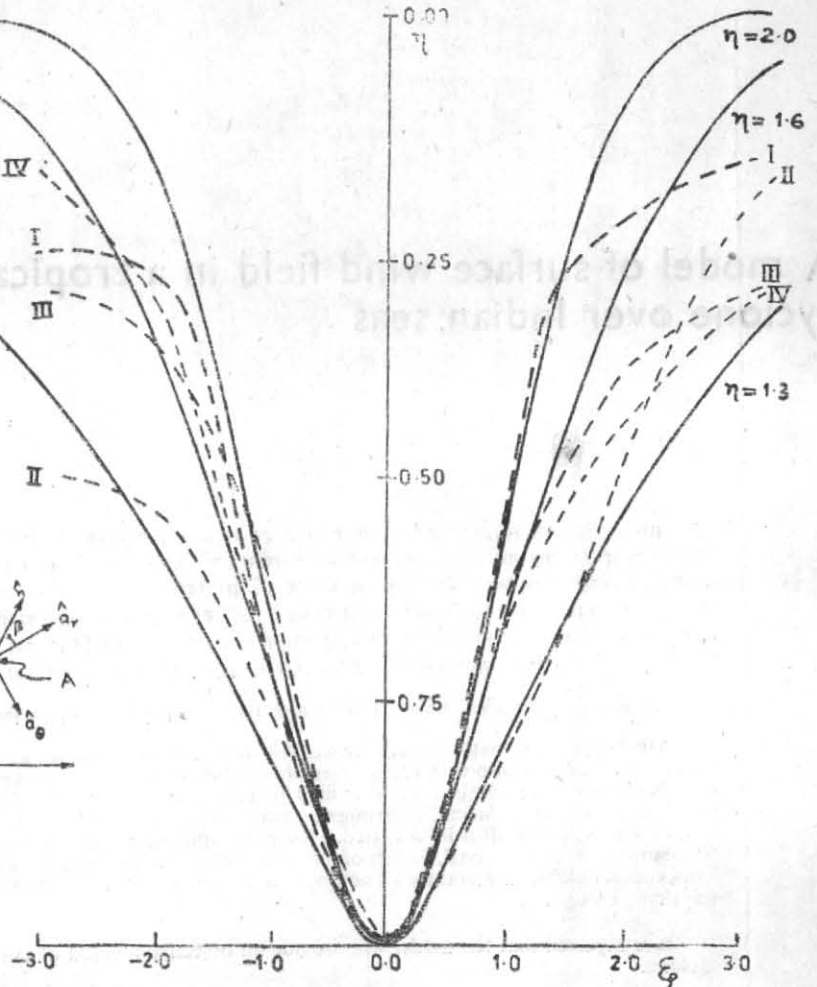


Fig. 2. Variation of normalized pressure drop with normalized distance for different values of  $n$ . Broken curves I, II, III, IV, are actual variations as observed in the False Point cyclone of September 1985, the Contai cyclone of September 1976, the Masulipatnam cyclone of October 1949 and the Cuddalore cyclone of December 1972 respectively

field. instantaneous wind speed and cross-isobaric angle at any point. In order to reduce the number of unknown some simplifying assumptions are made as discussed below.

### 2. Quasi-equilibrium wind

A parcel of air moving inside a cyclone field experiences acceleration as it encounters different pressure at different points in the trajectory due to two factors : (i) the cross-isobaric nature of the flow, and (ii) the motion of the pressure field itself in a moving cyclone. Thus the assumption of an equilibrium of all the forces acting on a parcel of air is not valid for motion inside a cyclone field. However, it is still possible for a parcel of air to acquire values of speed and cross isobaric angle close to that of the equilibrium wind if the change in pressure gradient force occurs slowly compared to the time taken by the parcel to adjust to the pressure gradient. Since the coriolis, centrifugal and friction forces depend on the speed of the parcel and always act to restore the wind speed towards the equilibrium wind

speed the adjustment process must be a quick one. This is also supported by computations of Myers and Malkin (1961) who showed that the acceleration term is one order smaller in magnitude than the driving forces. They further showed that any asymmetry in the wind field at outer edges of the cyclone is quickly damped out and has little effect inside. Thus, it is reasonable to assume that at any instant of time the speed of a parcel inside the cyclone field is close to the value obtained under assumption of equilibrium of forces.

An estimate of the relative importance of different terms in the equation of motion can be obtained by using the method of scale analysis. Such an analysis for flow within a cyclone field was done by Anthes (1974) mainly for the troposphere above the boundary layer. In what follows we attempt a similar analysis for the layer close to the surface. For this purpose the cyclone field is divided into two distinct regions — one consisting of the area from the outer periphery of the central calm 'eye' upto the outer boundary of the wall cloud, assumed to be 50 km from the centre of the cyclone (region A) and the other (region B) consisting of the area outside region A. Within the first region numerical values of all forces and the wind speed are one order of magnitude higher than those in the region B.

From computations of Myers and Malkin (1961) and also present computations it is seen that the cross-isobaric angle decreases within region B as one moves closer to the centre of the cyclone. This also follows from the equation of continuity if one assumes that vertical mass transport in the region B is small and the variation in air density can be neglected. Then considering the inflow into and outflow from an annulus region concentric with the centre of the cyclone we get

$$r V_r = \text{constant}$$

where,  $r$  = distance from the centre of the cyclone

$V_r$  = radial component of velocity of wind at distance  $r$  from the centre.

Since  $V_r$  is the product of wind speed  $V$  and sine of the cross-isobaric angle  $\beta$  and the wind speed is inversely proportional to the second or higher order of distance  $r$  from the centre, it follows that cross-isobaric angle increases with  $r$ .

In real cyclones vertical velocity is not zero within the region B and the radial velocity does not vary inversely with distance. Computed values of cross-isobaric angle suggest that the radial velocity remains more or less same even though the wind increases inwards by about 50 km hr<sup>-1</sup> across the region B. At the outer edge of the region B at about 250 km away from the cyclone centre the value of radial velocity is taken to be 10 km hr<sup>-1</sup> corresponding to a velocity of 20 km hr<sup>-1</sup> and cross-isobaric angle of 30 degrees. Across the region A radial velocity decreases till it becomes zero at the eye wall which is about 10 km outward of the cyclone centre. Hence, a value of 5 km hr<sup>-1</sup> is chosen as the representative radial velocity in this region.

TABLE 1

Order of magnitude of various expressions in the equations of motion

Quantity	Expression	Region A	Region B
Radial width (km)	$L$	40	200
Mean radial distance (km)	$R$	25	125
Time (hr)	$t = L/V_r$	8	20
Mean speed (km hr <sup>-1</sup> )	$V$	100	45
Change in speed across the region (km hr <sup>-1</sup> )	$\Delta V$	60	50
Change in cross-isobaric angle (degrees)	$\Delta \beta$	8	22
Tangential acceleration (km hr <sup>-2</sup> )	$\Delta V/t$	7.5	2.5
Normal acceleration (km hr <sup>-2</sup> )	$V \Delta \beta/t$	1.1	1.1
Pressure gradient (mb km <sup>-1</sup> )	$\Delta p/\Delta R$	0.500	0.025
Pressure gradient acceleration (km hr <sup>-2</sup> )	$\Delta p/\rho \Delta R$	650	32.5
Friction acceleration (km hr <sup>-2</sup> )	$k s V^2$	60	15
Coriolis acceleration (km hr <sup>-2</sup> )	$f V$	10	5
Centrifugal acceleration (km hr <sup>-2</sup> )	$V^2/R$	400	20
Acceleration due to storm motion (km hr <sup>-2</sup> )	$V V_c/R$	60	6.0

Under these conditions magnitudes of different forces are determined as presented in Table 1. It is seen that the inertial acceleration terms are atleast one order smaller than the main forces, namely, pressure gradient, friction and centrifugal forces. The coriolis force though of the same order as the acceleration term is retained as its effect is to reduce the cross-isobaric flow thus restoring equilibrium. However, it must be mentioned here that a solution of the complete equations of motion including acceleration terms can be obtained only when the pressure gradient, wind and cross-isobaric angle fields are completely known at some initial time from actual observations. In the absence of such observations the best that can be done is to neglect the acceleration terms and treat the problem as a steady state diagnostic one.

Even under the assumption of quasi-equilibrium the set of Eqns. (1) and (2) cannot be solved until one of the pressure gradient field, wind speed field or cross-isobaric angle field is known. Over Indian seas surface wind observations inside a cyclone field are restricted to a few ships' observations except for one case in 1976, analysed by Sivaramakrishnan and Mukherjee (1984), when a storm passed close to Oil and Natural Gas Commission (ONGC) off-shore oil rigs in the Arabian sea. Further, observed wind in a cyclone field consists of both the quasi-equilibrium wind discussed above and the smaller scale contributions like squalls, tornadoes, turbulent momentum exchange etc going on inside the cyclone. The pressure field is more stable as it is less distorted by small scale effects and may persist for a short time even after landfall. Hence, in the present study pressure field is taken as the input while the wind speed and cross-isobaric angles are computed from the above equations.

### 3. Pressure field inside a cyclone

Over sea areas observations of pressure inside a cyclone field are as few as those of wind. However, many storms originating over Indian sea areas have crossed coast in the severe cyclone stage. Some of the notable ones are the False Point (20° 20'N, 86° 45'E) cyclone of 1885, the Nellore (14° 27'N 79° 59'E) cyclone of 1927 and the Andhra Cyclone of 1977. Out of these, extensive records of pressure and wind are available for the cyclone in 1885 which crossed coast near the light house at False Point. The presence of a period of clear weather and calm wind between periods of gale wind from opposing directions indicates that the eye of the storm passed directly above the light house. The pressure profile, wind force in Beaufort scale and wind direction in sixteen points of compass are reproduced in plate 46 of *Bay of Bengal cyclone Hand book* by Elliot (1890).

An examination of the pressure profile of False Point cyclone and that of other cyclones suggests an exponential type of variation with distance which is symmetric about the location of minimum pressure. Mathematically such a variation can be expressed as :

$$p(r) = p_{\infty} - (p_{\infty} - p_0) \exp \left\{ -\frac{n-1}{n} \left( \frac{r}{a} \right)^n \right\} \quad (3)$$

where,  $p(r)$  = Pressure at a distance  $r$  from the centre of the storm

$p_{\infty}$  = peripheral pressure

$p_0$  = central pressure

$n$  = a variable in the power of the exponent

$a$  = distance at which pressure gradient is maximum

The above expression for pressure as a function of distance from the centre of the storm exhibits the following properties — (i) at great distances from the centre, pressure is equal to the peripheral pressure, (ii) at the centre, pressure is equal to the central pressure and (iii) at a distance 'a' from centre, pressure gradient is

maximum (since at  $r=a$ ,  $\frac{d^2p}{dr^2} = 0$  and  $\frac{d^3p}{dr^3} < 0$ )

The azimuthal asymmetry of the pressure field, however cannot be accounted for as the above expression is symmetric about the centre.

The dependence of the pressure field on  $n$  can be better understood by expressing Eqn. (3) in non-dimensional form :

$$\eta = \exp \left\{ -\frac{n-1}{n} \xi^n \right\}, \text{ where } \eta \text{ is the}$$

fractional pressure drop [ $\eta = (p - p(r))/(p_{\infty} - p_0$ ]

and  $\xi (=r/a)$  is the non-dimensional distance. These non-dimensional coordinates are similar to those used by Fletcher (1955). The value of  $n$  should be greater than one as otherwise pressure defect either remains same ( $n=1$ ) or increases away from the centre of the storm. The extent of the pressure field depends on the value of  $n$  in the sense that the distance at which the fractional pressure defect attains a particular value depends on the value of  $n$ . In Fig. 1(b) values of  $\xi$  for which  $\eta$  is equal to .01 and .50 are plotted for different values of  $n$ . By comparison with actual observations it is seen (Fig. 2) that the value of  $n$  lies between 1.3 and 2.0. In the present paper computations are done by taking various values for  $n$  between 1.5 and 2.0.

### 4. Wind speeds and cross-isobaric angles inside a cyclone field

Once the pressure field inside a cyclone is approximated by Eqn. (3), wind speed and cross-isobaric angle at any point can be determined by solving simultaneously the following equations :

$$\frac{1}{\rho} \frac{\partial p}{\partial r} \sin \beta - k_s V^2 = 0 \quad (4)$$

$$\frac{1}{\rho} \frac{\partial p}{\partial r} \cos \beta - fV - \frac{V^2}{r} \cos \beta + \frac{V V_c}{r} \sin \theta - k_n V^2 = 0 \quad (5)$$

These are simplified forms of Eqns. (1) and (2) obtained under assumptions of quasi-equilibrium of forces and azimuthal symmetry of the pressure field. For the purpose of actual computations, the cross-isobaric angle is eliminated from Eqn. (5) by making use of Eqn. (4) and the resultant polynomial in wind speed is solved by using the Bolzano bisection method. The value of cross-isobaric angle is easily obtained from Eqn. (4) once the value of wind speed is known.

Both wind and cross-isobaric angle fields depend on values of friction parameters  $k_s$  and  $k_n$  and also on the direction and speed of the cyclone. In their work Myers and Malkin (1961) have assumed values of .01250  $\text{km}^{-1}$  and .01375  $\text{km}^{-1}$  respectively for  $k_n$  and  $k_s$  and obtained values close to 35 degrees for the maximum cross-isobaric angle within the cyclone field.

In the present model, however, for same value of  $k_s$  and  $k_n$  maximum cross-isobaric angle within the storm field is found to be in excess of 45 degrees in some cases while the maximum wind is less than that obtained from the empirical formula of Mishra and Gupta (1976). From a series of numerical experiments done with different values of friction parameters it was found that good agreement with observations over Indian area is achieved for values of .00600  $\text{km}^{-1}$  and .00525  $\text{km}^{-1}$  for  $k_s$  and  $k_n$  respectively. These values are used for all subsequent computations,

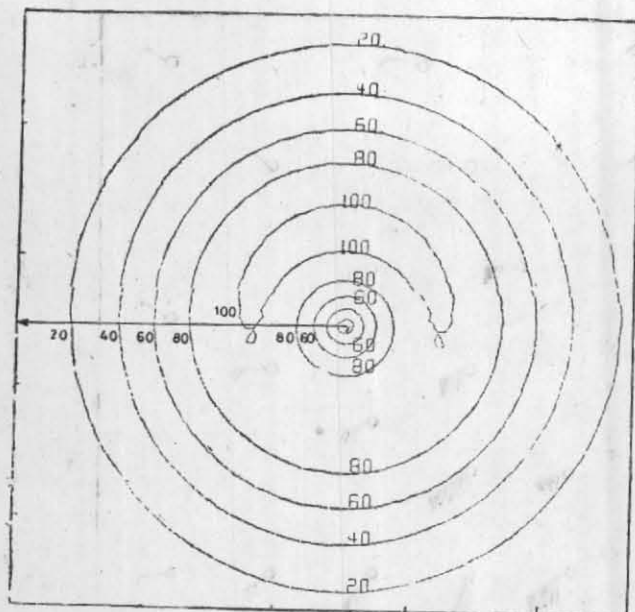


Fig. 3. Computer drawn isotachs (in kt) of the model derived wind field of a cyclone over the Arabian Sea located at  $14.7^{\circ}$  N and  $60.1^{\circ}$  E on 24 May 1963 and pressure drop of 59 mb. The direction of motion of the cyclone is indicated by an arrow

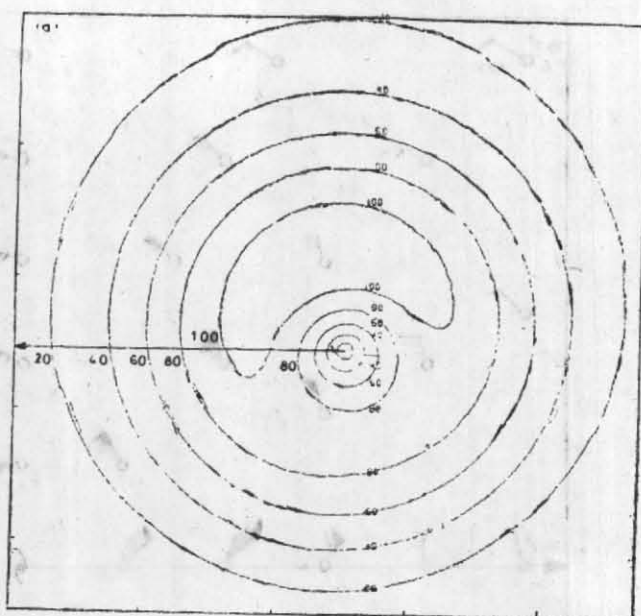


Fig. 4(a). Computer drawn isotachs of the resultant wind field obtained by combining the wind field in Fig. 3 with an ambient climatological wind field

It may be mentioned here that there is no reason to believe that surface friction parameters are constant throughout the whole of the cyclone field as the state of the sea varies from location to location—waves of greater height being predominant near the region of maximum wind. However, in the absence of any detailed observation of wind field inside a cyclone forming over Indian seas it is futile at the present stage to attempt further sophistication in the modelling of friction parameters.

The effect of friction on wind field is to decrease the wind speed and to increase the cross-isobaric angle. In the absence of friction no cross-isobaric flow is possible in a steady-state cyclone. As a consequence convergence into the storm field and associated vertical motion disappear thus cutting off the energy source due to the release of latent heat of condensation.

Even though the assumed pressure distribution is axisymmetric, the wind and cross-isobaric angle fields are not so, as the coriolis and cyclone motion terms in Eqn. (5) are not symmetric. The asymmetry introduced through the coriolis term, however, is small as the latitudinal extent of cyclonic storms is not large and the magnitude of coriolis force is one order smaller than other forces associated with such cyclones. Thus, in the present model asymmetry in the wind field is essentially due to the motion of the cyclone. Within the cyclone field winds are stronger in the half to the right of the direction of motion compared to those in the half to the left. This is due to the fact that in the right hand side half,  $\sin \theta$  is positive and hence the effect of cyclone motion adds to the effect of pressure gradient force.

Fig. 3 gives the computer-drawn isotach field of the model derived wind field of the cyclone over the Arabian Sea at  $14.7^{\circ}$  N and  $60.1^{\circ}$  E. On 24 May 1963 the central pressure drop of this cyclone was 59.0 mb as measured by reconnaissance aircraft (Mishra and Gupta 1976). The cyclone's speed of propagation to west was  $15 \text{ km hr}^{-1}$  and the radius of maximum wind is estimated to be 33 km. The maximum wind speed as computed on the basis of the present model is 104.3 kt, quite close to the observed value of 104.0 kt; it is located in the right half with respect to the cyclone motion and slightly to the rear of the centre of the cyclone.

The model gives us the wind field due to the pressure distribution associated with the cyclone. However, if the cyclone is viewed as a vortex embedded in the ambient atmospheric flow caused by semi-permanent pressure field, e.g., sub-tropical high pressure cells, the actual wind at any point will be a resultant of contributions from the ambient field and the cyclone. Fig. 4(a) is the computer-drawn isotachs for the resultant wind field.

Fig. 4(b) is the resultant wind field for the above described cyclone as plotted by hand. This wind field is obtained by vectorially adding a constant ambient field of  $070^{\circ}/10$  knots wind to that due to the cyclone. The maximum wind speed in this case increases to 110.0 kt with little change in its location. The ENE'y 10 knots wind is assumed as the average climatological surface wind over Indian seas during cyclone seasons.

##### 5. Maximum wind inside a cyclone field

One of the more important features of a cyclone is the existence of a ring of maximum winds beyond

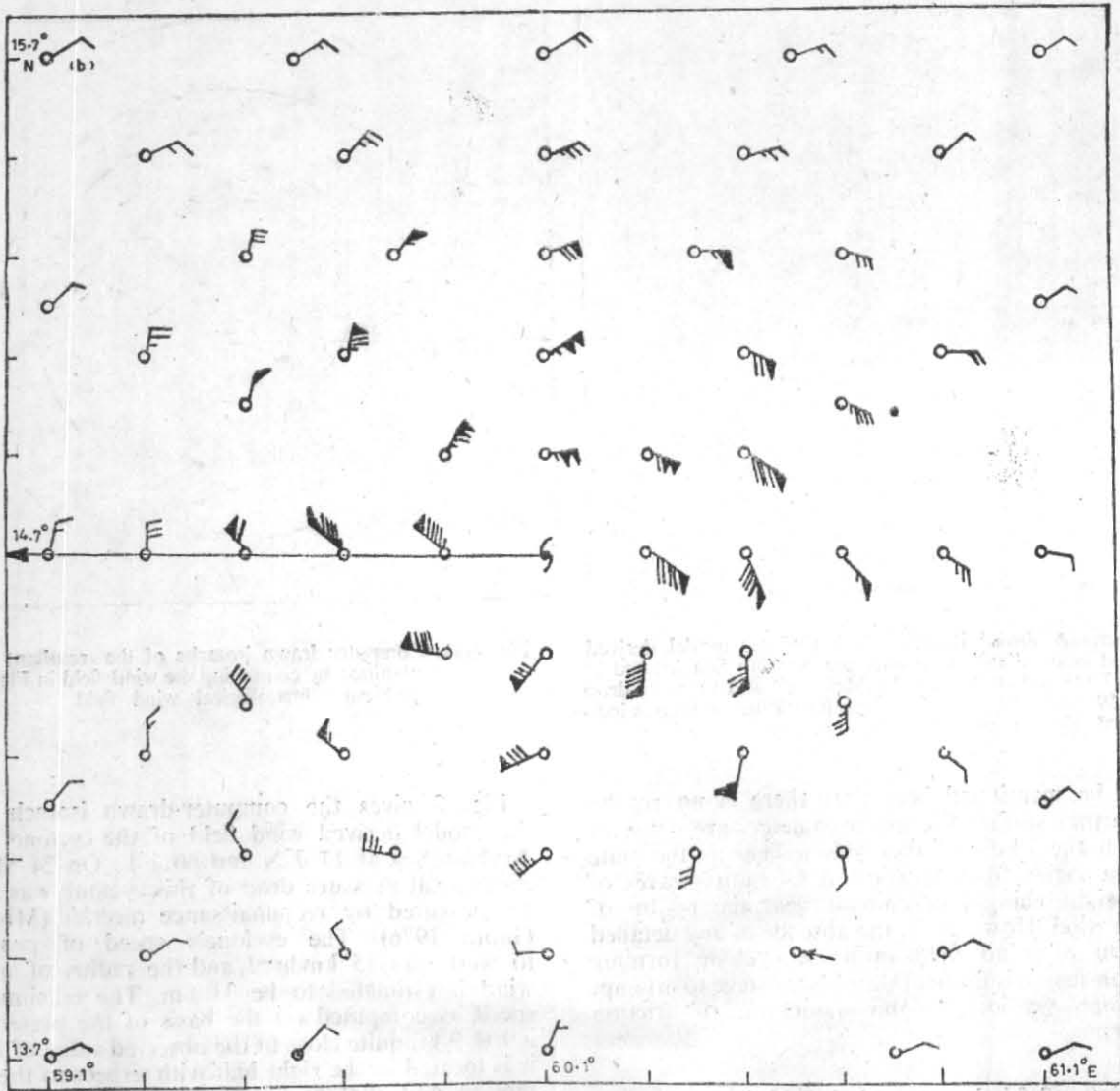


Fig. 4(b) Hand drawn wind vectors of the wind field presented in Fig. 4(a)

the central calm area. Estimation of the magnitude of the maximum wind and its distance from the storm centre is of practical importance in the prediction of wave heights and surges associated with storms. The wind field itself is important for shipping.

In the absence of friction an expression for wind speeds inside the cyclone field can be obtained in the form

$$V = -a + \left( a^2 + \frac{r}{\rho} \frac{\partial p}{\partial r} \right)^{\frac{1}{2}} \quad (6)$$

where,  $2a = fr - V_c \sin \theta$

The above expression is obtained from the following equation (gradient wind) expressing balance of forces in the absence of friction :

$$\frac{1}{\rho} \frac{\partial p}{\partial r} - fV - \frac{V^2}{r} + \frac{VV_c \sin \theta}{r} = 0 \quad (7)$$

The distance from the centre of the cyclone at which the wind speed has maximum magnitude can be obtained from Eqn. (6) by equating the first derivative of wind speed to zero. Neglecting the effect of coriolis force a simple expression can be obtained for the radius of maximum wind  $r_0$  in the form :

$$p' + r_0 p'' = 0 \quad (8)$$

where  $p'$  and  $p''$  are respectively the first and second derivatives of pressure with respect to distance from the centre of the storm. Substituting Eqn. (3) for pressure inside a cyclone field we get

$$r_0 = \left( \frac{n}{n-1} \right)^{\frac{1}{n}} a \quad (9)$$

where  $a$  is the radius of maximum pressure gradient. It has been verified that for the above value of  $r_0$  the second derivative of  $V$  in Eqn. (6) becomes negative satisfying the other condition for  $V$  to be maximum. It is evident from the above expression that strongest

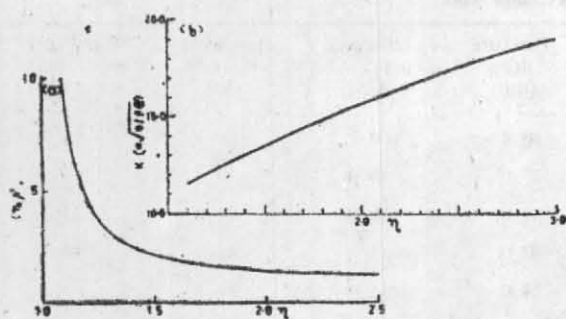


Fig. 5(a). Variation of the ratio of radii of maximum pressure gradient for different values of  $n$

Fig. 5(b). Variation of  $k$  with  $n$

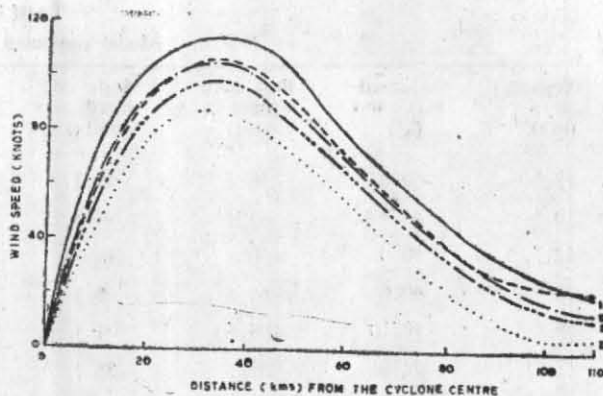


Fig. 6. Variation of model wind derived wind speed with distance in directions to the right (I), to the left (II), to the rear (III) and ahead (IV) of the direction of motion. The curve in broken lines represents the variation based on all instrumental observations of wind recorded on the three oil rigs through which the cyclone passed. All curves are for the case of the Gopnath ( $21^{\circ} 12' N, 72^{\circ} 07' E$ ) cyclone of May/June 1976

pressure gradients occur closer to the centre of the storm than the belt of maximum wind. This separation of the belt of maximum wind from the region of maximum pressure gradient is a characteristic of the cyclostrophic flow in contrast with the geostrophic flow in which maxima in pressure gradient and wind fields coincide. In Fig. 5(a) variation of the ratio ( $r_0/a$ ) for different values of  $n$  is shown. For the pressure profile used by Myers and Malkin (1961) the belt of maximum wind appears at a distance twice that of the maximum pressure gradient.

Substituting expressions for  $r_0$  and  $\left(\frac{\partial p}{\partial r}\right)$

from Eqn. (9) in Eqn. (6), we get an expression for the maximum wind in the form :

$$V_{\max} = \frac{1}{2} V_c \sin \theta + \left\{ \left( \frac{1}{2} V_c \sin \theta \right)^2 + n \Delta p / (\rho e) \right\}^{\frac{1}{2}} \quad (10)$$

In the case of a stationary storm the above expression reduces to a form similar to that of Fletcher (1955)

$$V_{\max} = k \sqrt{\Delta p}$$

where,  $k = \sqrt{n/(\rho e)}$  has the dimension of  $M^{-\frac{1}{2}} L^{\frac{3}{2}}$

Within the ring of maximum winds strongest and weakest winds occur in directions normal to the direction of motion of the cyclone and respectively to the right ( $\theta = 90^{\circ}$ ) and left ( $\theta = 270^{\circ}$ ) of it. The difference in these wind speeds is equal to the speed of the storm. This is obtained by putting  $\theta$  equal to  $90^{\circ}$  and  $270^{\circ}$  in Eqn. (10). In Fig. 6 the model derived wind speeds are plotted against distance from the centre in the case of the Gopnath ( $21^{\circ} 12' N, 72^{\circ} 07' E$ , Sivaramakrishnan and Mukherjee 1984) cyclone of May/June

1976 and compared with actual winds recorded by ONGC rigs over the Arabian Sea.

For a stationary cyclone the numerical value of the factor  $k$  connecting the magnitude of maximum wind to the square root of the pressure drop at the centre of the storm depends on the value of  $n$ . The larger the value of  $n$ , i.e., the tightness of the pressure profile, the stronger is the maximum wind. The variation in the value of the factor  $k$  for different values of  $n$  is shown in Fig. 5(b).

The effect of storm motion is to increase the value of  $k$ . For a storm with central pressure drop of 50 mb, the value of  $k$  increases by about 1 if the storm is moving with a speed equal to 14 knots. The effect of storm motion on  $k$  is more pronounced for storms with less central pressure drop and vice versa. For cyclones over Indian seas, Mishra and Gupta (1976) have obtained a numerical value of 14.2 for  $k$  by analysing 35 observations pertaining to 29 cyclones. Assuming that the mean pressure drop and speed of translation of the cyclones sampled by Mishra and Gupta were 25 mb and 7 knots respectively we obtained a value of 1.5 for  $n$  corresponding to the above value of  $k$ . This value of  $n$  is smaller than that obtained from comparison of actual pressure profiles of cyclones because of the fact that frictional effects were neglected in deriving Eqn. (10).

In Table 2 we present the model computed values of maximum wind for 50 cases pertaining to 44 cyclones. Observed values of maximum wind as reported by Mishra and Gupta (1984) and values obtained from Fletcher's formula by using a least square fit value of 14.14 for  $k$  are also presented for comparison. The

TABLE 2  
Model computed maximum wind

Pressure drop (mb)	Observed max. wind (kt)	Best least square fit (kt)	Model computed max. wind (kt)	Pressure drop (mb)	Observed max. wind (kt)	Best least square fit (kt)	Model computed max. wind (kt)
12.6	60.0	50.2	49.3	40.0	100.0	89.4	85.9
10.3	45.0	45.4	44.8	25.0	80.0	70.7	69.0
12.7	50.0	50.4	49.8	35.0	110.0	83.7	80.3
23.0	60.0	67.8	66.3	10.0	45.0	44.7	44.7
59.0	104.0	108.6	104.3	24.0	85.0	69.3	67.2
17.7	70.0	59.5	58.2	29.0	100.0	76.2	73.6
21.4	60.0	65.4	63.3	12.3	65.0	49.6	49.5
32.5	80.0	80.6	77.4	25.0	80.0	70.7	69.0
27.0	80.0	73.5	71.7	22.0	75.0	66.3	64.8
23.6	60.0	68.7	67.7	10.0	45.0	44.7	44.2
13.7	50.0	52.3	52.3	25.5	74.0	71.4	69.7
32.0	85.0	80.0	78.0	15.0	55.0	54.8	54.1
21.8	50.0	66.0	64.4	21.9	55.0	66.2	64.0
49.0	115.0	99.0	95.7	34.0	91.0	82.5	79.2
42.9	70.0	92.6	89.5	11.8	50.0	48.6	48.0
34.5	60.0	83.1	80.3	34.5	80.0	83.1	79.8
23.5	50.0	68.6	66.9	20.0	55.0	63.2	61.7
9.0	50.0	42.4	41.9	20.0	75.0	63.2	62.2
36.8	75.0	85.8	82.9	67.0	104.0	115.8	111.2
34.8	80.0	83.4	80.6	21.0	59.0	64.8	62.8
12.7	50.0	50.4	49.5	53.0	100.0	103.0	98.9
25.4	80.0	71.3	68.9	32.0	70.0	80.0	77.3
15.2	50.0	55.1	54.0	20.0	70.0	63.2	61.7
13.1	46.0	51.2	50.2	22.7	55.0	67.4	65.1
19.5	55.0	62.4	60.5	44.0	100.0	93.8	90.1

Values in column three are calculated from the equation  $V_{\max} = 14.142 \sqrt{\Delta p}$  while those in column four are computed for  $a=20$  km,  $R_m=30$  km and translation speed for cyclone  $=15$  km hr<sup>-1</sup>.

model computed values of maximum wind for a fixed value of radius of maximum wind equal to 30 km and fixed translational speed equal to 15.0 km hr<sup>-1</sup> have a root mean square error equal to 10.95 kt while the best fit Fletcher type formula produces a rms error equal to 10.76 kt for the above sample. The model is expected to do better than statistics when satellite derived values of radius of maximum wind and translation speed are given as inputs.

Since the parameters of a cyclone quite often undergo rapid changes it is necessary to have a nomogram covering probable ranges of each individual parameter influencing the wind field. To facilitate quick computations for operational forecasting such a nomogram is constructed and presented as Fig. 7. In this figure the ordinate gives the maximum wind speed while the stepped abscissae (I to V) give the central pressure drop corresponding to values of radius of maximum pressure gradient equal to 5 km, 10 km, 15 km, 20 km and 25 km respectively. For each value of radius of maximum pressure gradient two curves are drawn

corresponding to translational speed of the cyclone equal to 5 km hr<sup>-1</sup> and 30 km hr<sup>-1</sup> respectively. Since these two curves are fairly close to each other, values of maximum wind corresponding to intermediate values of translational speed of the cyclones can be determined from them by interpolation. All the above curves correspond to a fixed value of  $n$  equal to 1.7. In terms of radius of maximum winds, which is more familiar to meteorologists, the curves I to V correspond to 7.5 km, 15 km, 22.5 km, 30 km and 37.5 km respectively.

## 6. Results

An analysis of observations from within the cyclone field and model computed values of pressure and wind shows the following :

- (i) The pressure distribution within cyclones originating over Indian seas can be approximated by Eqn. (3) for values of  $n$  between 1.3 and 2.0.



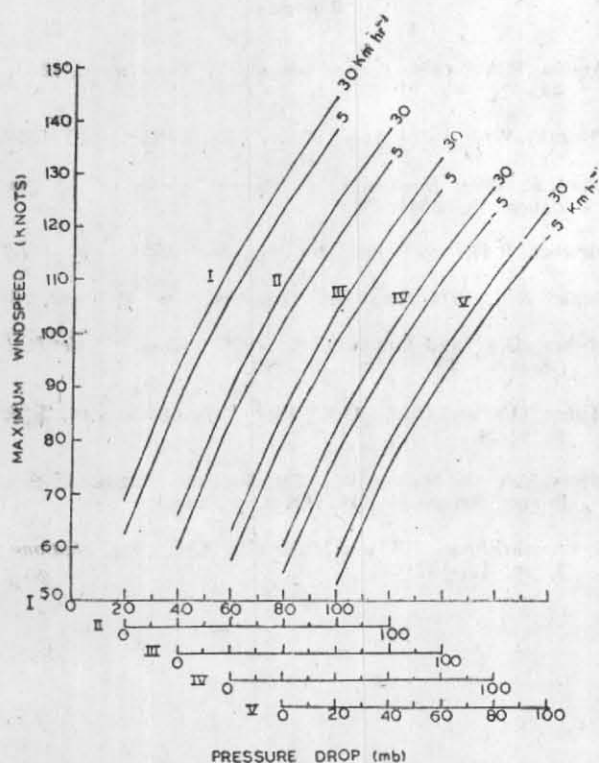


Fig. 7. A nomogram relating maximum wind speed with pressure drop for various radii of maximum pressure gradient and cyclone translation speed. Curves I to V represent radii of 5, 10, 15, 20 and 25 km respectively. Corresponding values of radius of maximum wind are 7.5, 15.0, 22.5, 30.0 and 37.5 km respectively

- (ii) A scale analysis of different forces shows that close to the ground inertial accelerations are one order of magnitude smaller than other terms.
- (iii) An asymmetry in the wind field is introduced due to storm motion even when the pressure field is axisymmetric.
- (iv) Observed maximum winds in cases of thirty-seven cyclones agree well with values computed from model equations with the value of  $n$  equal to 1.7.
- (v) The zone of maximum wind always lies further away from the cyclone centre than the region of maximum pressure gradient. A mathematical relationship between these two distances can be derived under the assumption of balance between pressure gradient, centrifugal and storm motion forces.
- (vi) For the same radius of maximum pressure gradient, spatial extent of the cyclone field decreases as the value of  $n$  increases. As  $n$  increases, the maximum wind strength also increases and the zone of maximum

wind moves towards cyclone centre. Thus in intensifying cyclones the radius of maximum wind decreases.

- (vii) The cross-isobaric angle increases outward from the centre of the cyclone. For the value  $.006 \text{ km}^{-1}$  for the tangential coefficient of friction  $k_s$ , the maximum cross-isobaric angle is about 20 degrees while for  $k_s = .013 \text{ km}^{-1}$  the latter increases to about 30 degrees.
- (viii) For same value of  $n$  and pressure drop at the centre, maximum values of pressure gradient and wind speed decrease as radius of maximum pressure gradient ' $a$ ' increases.
- (ix) The strength of the maximum wind increases with the motion of the storm. The amount of increase in maximum wind depends inversely on the pressure drop at the centre. As a consequence fractional increase in maximum wind is very pronounced in the case of cyclones with small pressure drop at the centre.

It may be mentioned here that values of parameters like  $n$ ,  $a$  and friction coefficients used in the model have been obtained by comparison with actual observations. In view of the paucity of observations from within cyclone field at present it may be necessary to modify these values when extensive observations from aircraft reconnaissance over Indian sea areas are available.

## 7. Conclusions

The present study shows that it is possible to map the wind field over high seas if the pressure drop at the centre of the cyclone and radius of maximum wind are known. Recent studies [Dvorak (1975) and Mishra and Gupta (1976)] have demonstrated that it is possible to estimate the pressure drop from satellite cloud imagery.

In the absence of dropsonde measurements from aircraft reconnaissance only an indirect method for the estimation of radius of maximum wind is possible. The method may be thought of as a corollary of the work of Gentry (1973). He has presented a diagram (not reproduced) relating temperature, pressure and wind speed in a hurricane with distance from its centre based on data collected from many aircraft reconnaissance flights through real hurricanes. It is apparent from the diagram that the location of maximum winds coincides with the centre of wall clouds. Since wall clouds associated with cyclones can be identified in satellite imagery by the technique of temperature contouring an estimate of the radius of maximum wind can be obtained by averaging in several directions. A fairly reliable value of the radius of maximum wind can be obtained from radar pictures when a cyclone comes under coast based cyclone radar surveillance.

As a result of comparison of actual observations with model derived wind field we have arrived at the conclusion that the assumption of quasi-equilibrium of forces leading to a steady state, though an approximation, is a powerful diagnostic tool for estimating the wind field inside a cyclone even when it is over the sea.

For operational forecasting purposes the computer printouts of isotach fields can be transmitted on facsimile to the field forecasting offices, viz., Cyclone Warning Centres and Area Cyclone Warning Centres.

#### Acknowledgements

The authors are thankful to S/Shri R. K. Bansal for plotter package, C. M. Pippal and Subash Chander for help in preparation and drafting of some diagrams and to Km. Jalaja for typing.

#### References

- Anthes, R.A., 1974, *Rev. of Geophys. & Space Phys.*, **12**, 3, pp. 495-522.
- Dvorak, V.F., 1975, *Mon. Weath. Rev.*, **103**, 5, pp. 420-430.
- Elliot, J., 1890, *Hand-book of cyclonic storms in the Bay of Bengal*, India Met. Dep.
- Fletcher, R.D., 1955, *Bull. Am. Met. Soc.*, **36**, 6, pp. 247-250.
- Gentry, R.C., 1973, *Proc. Reg. Trop. Cyc. Sem.*, Brisbane, 53-67.
- Mishra, D.K. and Gupta, G.R., 1976, *Indian J. Met. Hydrol. Geophys.*, **27**, 3, pp. 285-290.
- Mishra, D.K. and Gupta, G.R., 1984, *Vayu Mandal*, **14**, 1 & 2, pp. 18-24.
- Myers, V.A. and Malkin, W., 1961, National Hurricane Research Project, Report No. 49, U.S. Dep Comm.
- Sivaramakrishnan, T.R. and Mukherjee, A.K., 1984, *Mausam*, **35**, 2, pp. 181-182.